EVALUATION OF IMPACT DAMAGE IN COMPOSITE STRUCTURES USING ULTRASONIC TESTING

Angelika Wronkowicz-Katunin[1*], Krzysztof Dragan[2]

[1] *Silesian University of Technology, Institute of Fundamentals of Machinery Design, Konarskiego 18A, 44-100 Gliwice, Poland*
[2] *Air Force Institute of Technology, Laboratory of Non-Destructive Testing, Ks. Bolesława 6, 01-494 Warsaw, Poland*

* angelika.wronkowicz-katunin@polsl.pl

Abstract

Barely visible impact damage is one of the problems commonly occurring in composite elements during an aircraft operation. The authors described the mechanisms of impact damage formation and propagation in composite structures. The paper presents a performed analysis of an influence of impact parameters on the resulting damage, i.e. its detectability by means of visual observation as well as its extent determined based on ultrasonic tests results. The tests were conducted on the CFRP specimens with a wide range of impact damage cases obtained with combinations of variable impact energy and shapes of impactors. Additionally, an algorithm based on image processing and image analysis methods is proposed for the purpose of the effective evaluation of the ultrasonic data obtained.

Keywords: impact damage, composite structures, non-destructive testing, ultrasonic testing, image analysis

1. INTRODUCTION

Owing to their numerous advantages, polymeric composite materials are nowadays widely applied in manufacturing aircraft structural components. However, due to their complex nature and anisotropy, polymeric composites are vulnerable to the formation of various types of flaws during their production and damage during operation. One of the most significant problems is the type of damage caused by an impact, especially that of a low velocity. Damage occurring

in composite materials is a complex phenomenon and, under load, may propagate and interact with manufacturing defects up to failure. Because of that, composites are inspected with the use of non-destructive testing and evaluation (NDT&E) methods to detect the appearance of damage and monitor its progression.

The maintenance procedures regarding aircraft elements are accomplished according to one of developed to-date design methodologies. Historically, the development of these methodologies was motivated by several tragic accidents in the aircraft industry and the necessity to enhance safety and extend airworthiness [1]. One of the currently used approaches is based on the damage tolerance methodology, where the existence of small cracks and defects in the aircraft structure is permissible as long as the structure can resist failure before the scheduled inspection. The inspection intervals are therefore computed such that no crack can grow to the critical size before the next inspection [2]. Therefore, one of the most important tasks in this methodology is to perform periodic non-destructive inspections of the critical aircraft elements.

An aircraft inspection can range from a preflight or postflight inspection, which is a casual "walk-around" to visually check the general condition of an aircraft and is delivered mainly by the flight crew, to a detailed inspection involving a complete disassembly and the use of complex inspection aids, delivered by the qualified engineering staff. Among many NDT&E methods, ultrasonic testing (UT) is one of the most commonly applied owing to its capability to detect various types of defects and damage inside composite elements and evaluate their location and geometrical properties. Principally, the output obtained as a result of such an inspection is in the form of ultrasonic data presenting levels of attenuation of the ultrasonic waves by particular areas of a tested structure. A change in that levels may indicate the presence of a defect or damage, but also noise or, for instance, an element embedded inside the structure, such as a stiffening rib or a rivet.

2. IMPACT DAMAGE

Fibre Reinforced Polymer (FRP) composites have the major drawback of being fragile and particularly sensitive to loads in the thickness direction, such as impacts, both during manufacturing and in-service. In the case of the aircraft elements, impact damage may be caused by hail, bird strikes in flight, runway debris impacts (during take-off and landing), or tools dropped during maintenance [3, 4, 5]. Impact damage is often classified as being of low-, medium-, or high-energy (or -velocity), depending on the impact parameters, or as BVID (Barely Visible Impact Damage), minor VID (minor Visible Impact Damage), and large VID, depending on the damage visibility during visual inspections [6]. The resulting damage mechanisms due to impact loading can be divided into four distinct categories: delamination, matrix cracking, fibre breakage and

total perforation [7]. The structural response of composites differs between variable velocity impacts. Under a low-energy impact, a structure may experience only an elastic phase without perforation, since composites are able to absorb impact energy owing to the polymeric matrix that distributes energy through the structure [8]. With high velocities, e.g. in the case of ballistic impacts, the impact event is so short that the structure does not respond in flexural or shear modes, but a complete penetration occurs. The NDT&E of aircraft structures is primarily needed to detect of damage produced by low-velocity impacts, that have the potential to create BVID likely to cause significant internal structural damage with little, if any, visible evidence of damage at the surface [9]. The delaminations and interlaminar matrix cracks caused by a low-velocity impact tend to be distributed through the composite in a pattern that resembles the branches of a pine tree (Fig. 1). When adjacent to the impact site, the damage is limited to a relatively small region, but it extends in size with increasing depth and typically reaches its maximum size near the back-wall of the composite [9].
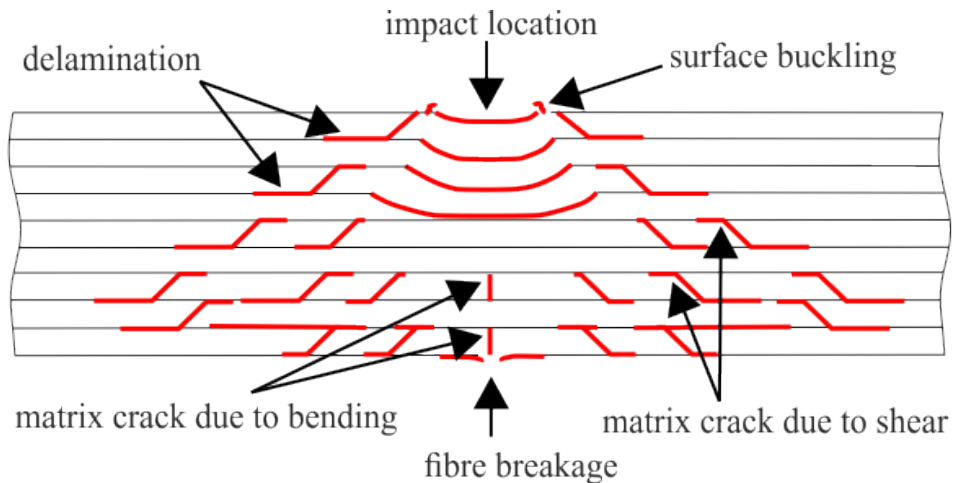

Fig. 1. A typical impact damage mode in FRP composite structures (adapted from [10])

Such BVID may grow during in-service and, if undetected, lead to catastrophic failure [8]. In the report [3], it is noted that in order to ensure BVID does not cause delamination resulting in structural failure, composite aircraft components are often designed with a safety factor of 3, or greater. Safety factors such as these have been employed in the design of major composite structures in the Boeing 787 Dreamliner, such as the fuselage.

84

3. MECHANISMS OF DAMAGE PROPAGATION IN COMPOSITE STRUCTURES

It should be pointed out that damage occurring in layered composites is a complex phenomenon and propagates progressively up to the failure. The failure of a polymer matrix composite is generally preceded by an accumulation of different internal micro- and macro-structural damage types. Normally, the damage is well distributed throughout the composite and progresses with an increasingly applied load. It coalesces to form a macroscopic fracture shortly before the catastrophic failure. The sequence and interaction of the failure mechanisms depend on a type of loading and properties of the constituents [11]. The three fundamental modes in which a composite may fail are tension, compression, and shear [5].

Based on the studies [12, 5], aimed at investigation of damage progression in a cross-ply laminated composite under fatigue loading, the stages under cyclic tension may look as follows. In the early stage of damage propagation, multiple matrix micro-cracking develops mainly in the layers with fibres aligned not parallel to the loading direction. As the cyclic loading continues, transverse matrix cracks develop from locations of defects such as voids, or areas of high fibre volume fraction or resin rich areas. Upon increasing loading, more and more cracks are formed. They grow and start interacting as they become closer, so that they become the macroscopic cracks. Stress concentrations cause initiation of so-called secondary cracks at the locations of plies adjacent to the ones with the primary cracks, and as a result – initiation of interfacial debonding and thus local interlaminar cracks. Merging of the interlaminar cracks into strip-like zones leads to large scale delaminations. This causes the loss of the integrity of the composite in the delaminated regions and further damage development resulting in an extensive fibre breakage. Finally, the fracture failure of the overall composite laminate occurs through the locally failed regions. In [12] it was reported that similar damage progression scenario occurs under quasi-static loading. Different orientation of plies in a laminate, varying thickness, or internal defects may modify the damage evolution [3, 13].

In view of this progressive damage behaviour, composite structures should be periodically inspected non-destructively to monitor the damage progression.

The purpose of the study presented in this paper was to investigate the dependency between impact parameters and the visibility of the resulting damage on the outer surface of elements inspected and the total area extent of the internal damage. In order to obtain a wide range of impact damage cases, various BVID scenarios were considered, i.e. different impact energies and shapes of impactors were used during the preparation of the specimens, which resulted in variable damage shapes and extents. The results were analysed both visually and using the UT method, which led to the results and conclusions presented in the following sections.

4. STRUCTURES AND EXPERIMENTS

The CFRP plates used in this study, purchased from Dexcraft s.c. (Poland), were manufactured with the resin infusion technology and tailored to specimens with the following nominal dimensions: 100×100×2.5 mm (width×length×thickness). The BVID was introduced artificially using a test rig for the drop weight impact tests (see Fig. 2), described in detail in [14]. In order to simulate various BVID configurations, the hemispherical impactors as well as the impactors with fixed granite stones were used. During the tests, seven types of impactors were applied, as presented in Fig. 2(c). With regard to aircraft structures, the use of these impactors enabled simulating impacts by hail, dropped maintenance tools, or runway debris of various sizes. It was assumed that the range of impact energy causing barely visible damage in the specimens used was in the range of 5–20 J, and the energy step of 2.5 J was established in the study. The combinations of seven impactor types and seven impact energy values gave 49 impact damage cases in total.
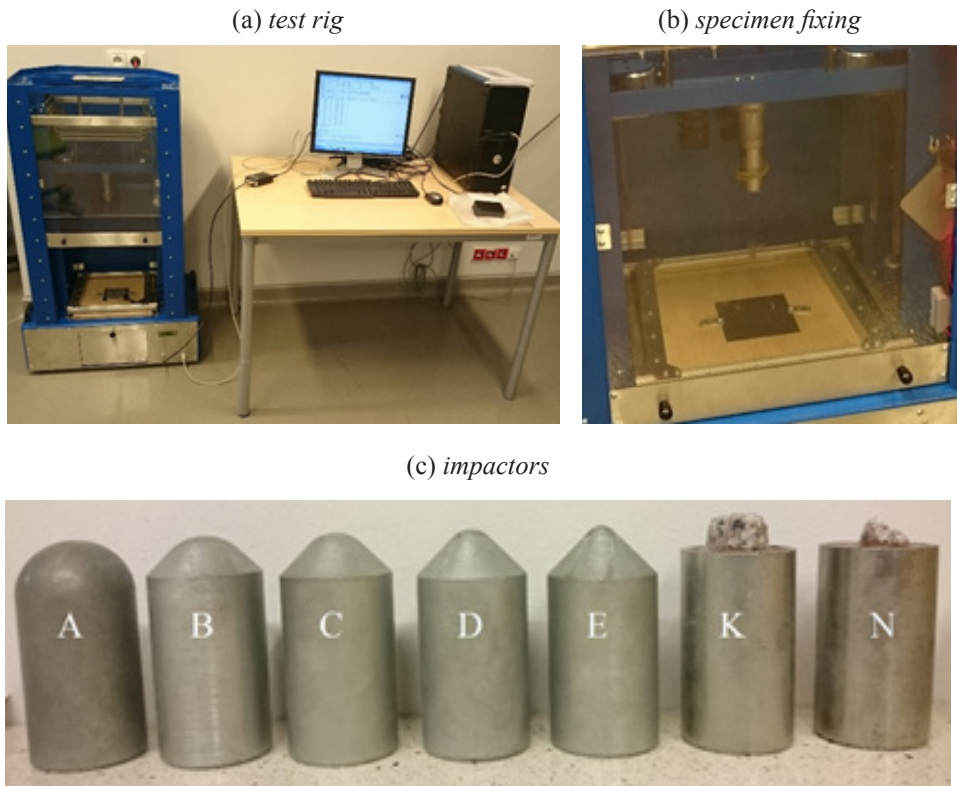
(a) *test rig*   (b) *specimen fixing*

(c) *impactors*

Fig. 2. Impact test rig (a,b) and used impactors (c) – hemispherical (radii R given in mm): A – R17, B – R14, C – R11, D – R8, E – R5, stone impactors: K – with flat surface, N – with rough surface

As expected, barely visible damage or no signs of potential damage could be noticed when visually observing the specimens' surfaces. The photographs of the specimens' surfaces after the impact are presented for selected cases in Fig. 3. It was observed that the impact signs were visible for the cases where the impactors with a rough surface (the impactors *K* and *N*) were used as well as for the cases of the impact energy of 15 J and above. For majority of the remaining cases, the visual inspection with the bare eye revealed no damage.
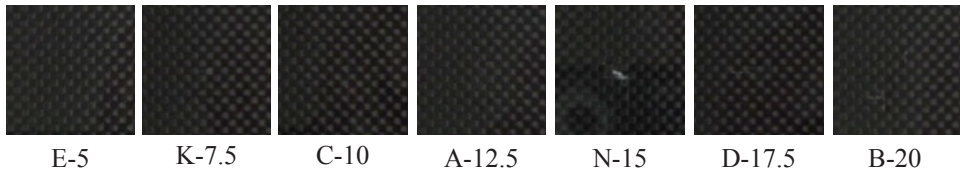

| E-5 | K-7.5 | C-10 | A-12.5 | N-15 | D-17.5 | B-20 |

Fig. 3. Exemplary photographs of the specimens' surfaces after impact (limited to the central areas of 35×35 mm)

Afterwards, the specimens were tested with the Pulse-Echo UT method using the MAUS® system with a transducer frequency of 5 MHz. The testing parameters were selected based on the comparative studies presented in [15]. The raw ultrasonic C-Scans obtained from the UT are presented in Fig. 4. These results reveal that the impacts introduced caused internal damage in all cases with the impact energies ranging between 7.5 and 20 J, whereas not in all cases with the impact energy of 5 J. It should be also noted that the specimens prepared allowed obtaining a variety of damage shapes including cracks and delaminations.

5. IMAGE ANALYSIS ALGORITHM

In order to calculate the total area surfaces of the resulting internal damage, an algorithm based on image processing and the analysis methods was elaborated. Selected steps of this algorithm prepared for the BVID evaluation, for the specimen case *K-15*, are presented in Fig. 5. The consecutive steps are detailed below. Firstly, the raw C-Scan is segmented using a developed MBP-based algorithm presented in [16]. The resulting image for the exemplary case is presented in Fig. 5(a). The aim of this step is to reduce data, which allows for further effective separation of the regions of interest (ROIs), i.e. damage, from the background. Then, the segments presenting undamaged regions are indicated to be removed from the image, i.e. assigned to zeros. This indication is reached by the interactive selection of one pixel point per one segment that is to be removed. The remaining regions (see Fig. 5(b)) indicate the presence of BVID but also the presence of a manufacturing flaw. For this reason, the next step is to select a final ROI by drawing a polygon around the damage location identified. This step

87

is interactive and relies on indicating the points of the polygon around the ROI (Fig. 5(c)). After that, the pixels outside the ROI are removed. The resulting image after this step is binarized by the assignment of ''ones'' to the non-zero pixels in order to extract the ROI contour and calculate its surface area. To enable visual verification if the BVID region was extracted properly, the boundaries of the final ROI are displayed on the input C-Scan (Fig. 5(d)).
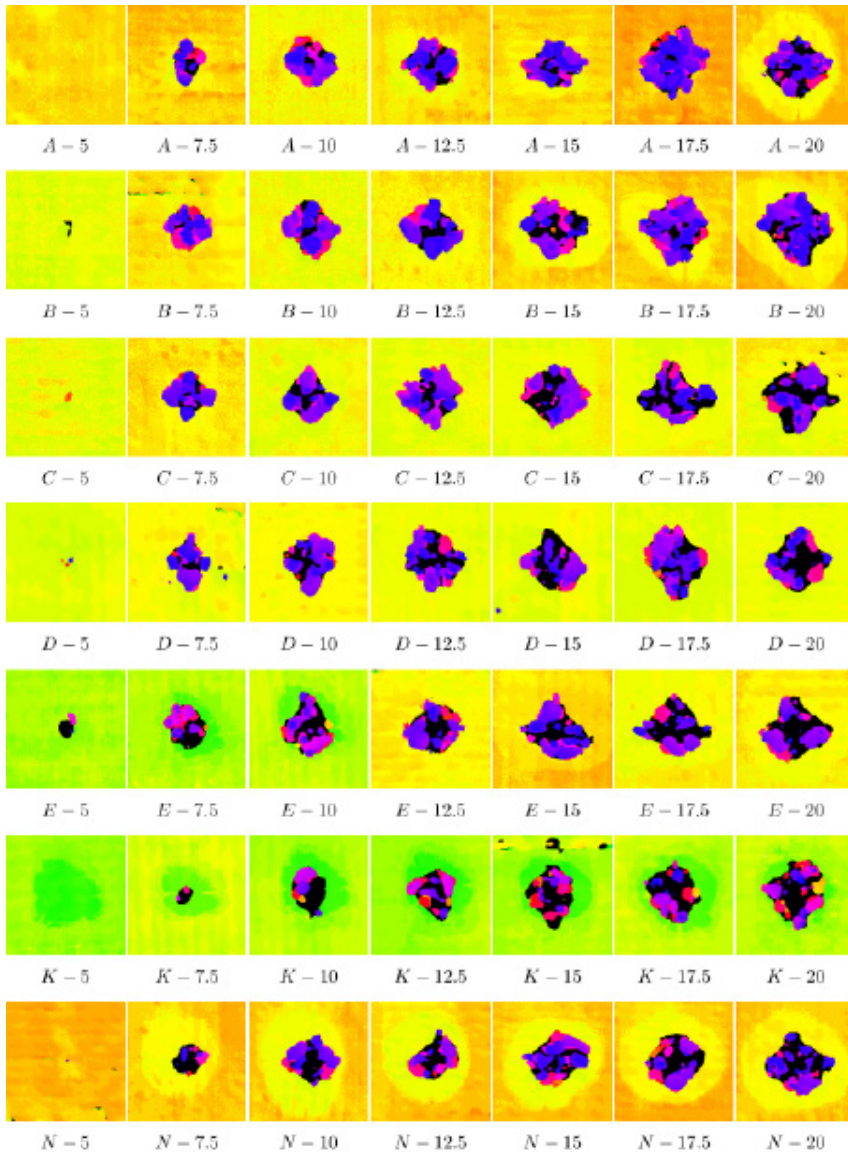

Fig. 4. Ultrasonic C-Scans of the impacted specimens (reduced to dimensions of 35×35 mm)
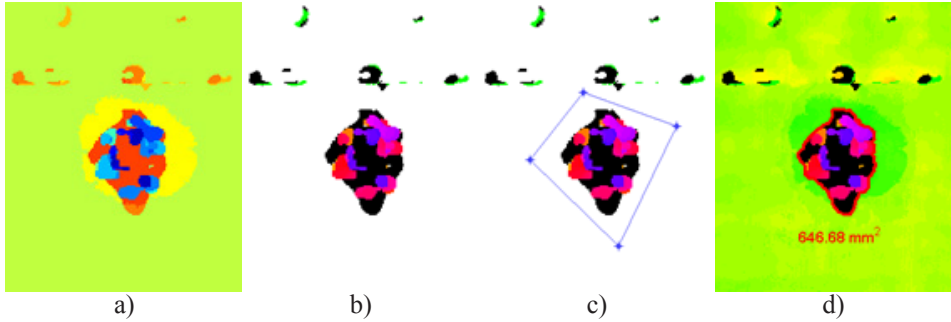
88

Fig. 5. Selected algorithm steps: image after segmentation (a), image after segments removal (b), ROI selection (c), input C-Scan with the BVID contour (d)

6. RESULTS AND DISCUSSION

All the C-Scans obtained were processed using the presented image analysis algorithm. The summary of the total area surfaces of the BVID is presented in Fig. 6.
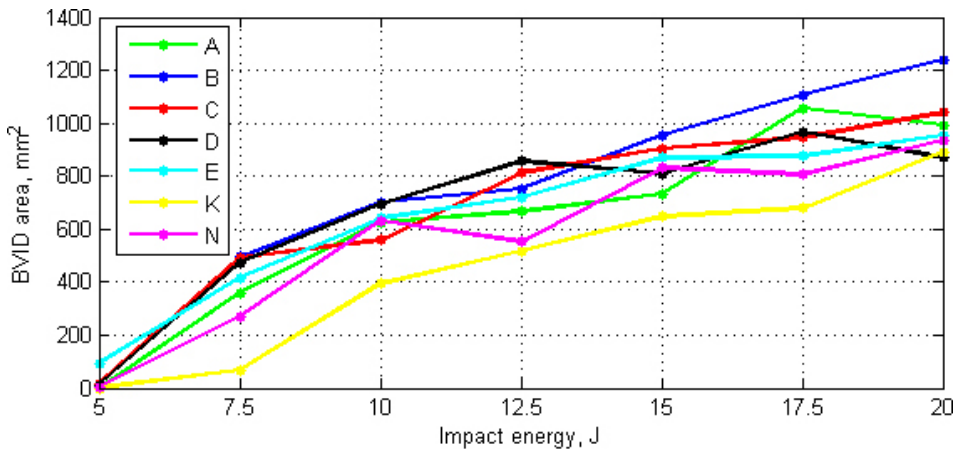

Fig. 6. Calculated BVID areas for the specimens impacted with variable energy values and impactor shapes (given in the legend of colours)

These results revealed that in the case of the impactors with the granite stones the more flat impactor *K* caused less damage for all the impact energy cases than the impactor *N* with the sharp ending. This was due to different types of stress distributions obtained when impacted with various shapes of impactor endings (flat solids caused mainly shear stress distribution whereas sharp shapes caused tension stress in the composite fibres and penetrated the matrix during the impact

89

[17]). For the cases impacted with the hemispherical impactors it was noted that the BVID produced by the impactor *A* was less than in the case of the impactor with a smaller radius *B* for all the impact energies, whereas for the remaining impactors with the decreased radius no clear dependency was observable.

Having regard to the visual analysis of the specimens after introducing the low energy impact damage one can also observe that internal damage of the total surface area of even ca. 800 mm^2 might be completely invisible on the outer side of the structure.

7. CONCLUSIONS

The presented study enabled performing the visual analysis as well as a qualitative evaluation of impact damage in CFRP structures with a thickness of 2.5 mm. For the latter purpose, an algorithm based on the image analysis methods was proposed. Based on the visual observation it was concluded that the impact signs were noticeable only for the cases of the impacts with a rough surface as well as for the cases of the impact energy of 15 J and greater. Based on the results of ultrasonic testing, it was concluded that impacts with the energy in the range of 7.5–20 J resulted in producing internal damage, whereas several specimens impacted with the energy of 5 J did not reveal any signs of damage. These results demonstrated the necessity of the application of non-destructive inspections of composite components since even large internal impact damage can be imperceptible when inspected visually.

The presented study is part of the on-going research. The next planned step is to develop a model-based method of a three-dimensional reconstruction of impact damage detected in C-Scans, which will allow evaluating the damage with respect to particular delaminated regions at various depth of the specimens.

8. ACKNOWLEDGEMENTS

9. REFERENCES

[1]   Wanhill R. (2003): *Milestone Case Histories in Aircraft Structural Integrity*, Comprehensive Structural Integrity 1, Elsevier: pp. 61-72.

[2]   Cot L. D., Bes C. and Gogu C. (2013): *Structural airframe maintenance strategy comparison: a new approach*. In: Structural Health Monitoring 2013: A Roadmap to Intelligent Structures: Proceedings of the Ninth International Workshop on Structural Health Monitoring, F.-K. Chang (Ed.). DEStech Publications, Inc: pp. 1460-1467.

[3] Taylor R. P. (2008): *Fibre composite aircraft – capability and safety*. Technical Report No. AR-2007-021. Australian Transport Safety Bureau.

[4] Hsu D. K. (2013): *15 – Non-destructive evaluation (NDE) of aerospace composites: ultrasonic techniques*. In: Non-Destructive Evaluation (NDE) of Polymer Matrix Composites, V. M. Karbhari (Ed.). Woodhead Publishing Series in Composites Science and Engineering. Woodhead Publishing: pp. 397-422.

[5] Giurgiutiu V. (2016): *Structural Health Monitoring of Aerospace Composites*. Academic Press.

[6] Bouvet C. and Rivallant S. (2016): *Damage tolerance of composite structures under low-velocity impact. Dynamic Deformation, Damage and Fracture in Composite Materials and Structures*. Woodhead Publishing: pp. 7-33.

[7] Donadon M. V., Iannucci L., Falzon B. G., Hodgkinson J. M. and de Almeida S. F. M. (2008): *A progressive failure model for composite laminates subjected to low velocity impact damage*. Computers & Structures 86(11): pp. 1232-1252.

[8] Meola C. and Carlomagno G. M. (2013): *14 – Non-destructive evaluation (NDE) of aerospace composites: detecting impact damage*. In: Non--Destructive Evaluation (NDE) of Polymer Matrix Composites, V. M. Karbhari (Ed.). Woodhead Publishing Series in Composites Science and Engineering. Woodhead Publishing: pp. 367-396.

[9] Rajic N. (2013): *13 – Non-destructive evaluation (NDE) of aerospace composites: flaw characterisation*. In: Non-Destructive Evaluation (NDE) of Polymer Matrix Composites, V. M. Karbhari (Ed.). Woodhead Publishing Series in Composites Science and Engineering. Woodhead Publishing: pp. 335-366.

[10] Shyr T.-W. and Pan Y.-H. (2003): *Impact resistance and damage characteristics of composite laminates*. Composite Structures 62(2): pp. 193-203.

[11] Gdoutos E. E. (2005): *Fracture Mechanics: An Introduction*. Vol. 123 of Solid Mechanics and Its Applications. 2nd edn. Springer Netherlands.

[12] Talreja R. and Singh C. V. (2012): *Damage and Failure of Composite Materials*. Cambridge University Press. New York.

[13] Huang J. Q. (2013): *2 – Non-destructive evaluation (NDE) of composites: acoustic emission (AE)*. In: Non-Destructive Evaluation (NDE) of Polymer Matrix Composites, V. M. Karbhari (Ed.). Woodhead Publishing Series in Composites Science and Engineering. Woodhead Publishing: pp. 12-32.

[14] Katunin A. (2015): *Impact damage assessment in composite structures based on multiwavelet analysis of modal shapes*. Indian Journal of Engineering and Materials Sciences 22: pp. 451-459.

[15] Wronkowicz A., Dragan K., Lis K. (2018): *Assessment of uncertainty in damage evaluation by ultrasonic testing of composite structures*. Composite Structures 203, pp. 71-84.

[16] Wronkowicz A. (2018): *Non-destructive evaluation of composite aircraft elements based on ultrasonic testing and image analysis*. Rozprawa doktorska. Politechnika Śląska, Gliwice.

[17] Katunin A. (2015): *Stone impact damage identification in composite plates using modal data and quincunx wavelet analysis*. Archives of Civil and Mechanical Engineering 15(1): pp. 251-261.